




Emergent organization and polarization due to active fluctuations

Benoît Mahault ^{1,*}, Prakhar Godara ¹, and Ramin Golestanian ^{1,2,†}

¹Max Planck Institute for Dynamics and Self-Organization (MPIDS), 37077 Göttingen, Germany

²Rudolf Peierls Centre for Theoretical Physics, University of Oxford, Oxford OX1 3PU, United Kingdom



(Received 24 March 2022; revised 24 February 2023; accepted 1 April 2023; published 12 April 2023)

We introduce and study a model of active Brownian motion with multiplicative noise describing fluctuations in the self-propulsion or activity. We find that the standard picture of density accumulation in slow regions is qualitatively modified by active fluctuations, as stationary density profiles are generally not determined only by the mean self-propulsion speed landscape. As a result, activity gradients generically correlate the particle self-propulsion speed and orientation, leading to emergent polarization at interfaces pointing either towards dense or dilute regions depending on the amount of noise in the system. We discuss how active noise affects the emergence of motility-induced phase separation. Our work provides a foundation for systematic studies of active matter self-organization in the presence of activity landscapes and active fluctuations.

DOI: [10.1103/PhysRevResearch.5.L022012](https://doi.org/10.1103/PhysRevResearch.5.L022012)

Introduction. Active matter refers to a broad class of systems driven out of thermal equilibrium at the level of their microscopic constituents. Although detailed balance can be broken locally in various ways, including the generation of local stresses [1,2], local production and consumption of chemicals [3], nonreciprocity in the interactions [4–9], or growth [10–12], systems composed of self-propelled particles play a central role in active matter studies [13–17]. An interesting feature of the latter case is that activity trivially couples to the particles' motion so that it can be used as a way to control the spatial dynamics of active systems with promising practical applications [18,19]. Spatial segregation of active particles can be achieved at the individual particle level, e.g., by imposing spatially varying self-propulsion speed [20–23], or at the collective level, by engineering quorum-sensing-type interactions triggering motility inhibition in single [24,25] and multicomponent [26] suspensions.

The physical principles leading to such controls apply to a wide class of systems and can thus be understood from minimal models, which most often deal with active Brownian particles (ABPs) [13]. ABPs are generally studied in the overdamped regime under the assumption that their self-propulsion speed relaxes on infinitesimal timescales so that it can be considered constant, and the stochastic dynamics of the self-propulsion velocity reduces to rotational diffusion. Actual active particles, on the other hand, self-propel as a result of intricate processes involving nontrivial timescales [27,28] and

usually evolve inside complex and noisy environments [29]. Moreover, individual measurements of active self-propulsion velocity often show it to be a dynamical fluctuating quantity [30–39], which is not a surprise given what we expect from mechanistic descriptions of self-propulsion. Phoretic colloids, for instance, are typically driven at their surface by a chemical reaction whose product density is a fluctuating quantity [28,40]. Low Reynolds swimmers, in turn, must self-propel by performing nonreciprocal cycles that may be described as stochastic transitions between internal states [41]. In both cases, fluctuations of the motility mechanism naturally lead to fluctuations in the self-propulsion speed. When the source of activity is inhomogeneous, e.g., in the presence of chemical product density or swimming medium viscosity gradients, such fluctuations can moreover vary in space.

Fluctuations of the active velocity, which hereafter we refer to as *active fluctuations*, must, by symmetry, carry independent contributions along the directions parallel and perpendicular to the self-propulsion direction. Unlike thermal noise, active noise is therefore multiplicative by design. Despite a few studies characterizing the statistical properties of active fluctuations [13,42–46], little is known about how the latter can in turn affect the spatial organization of the particles.

Here, we propose a formulation of fluctuating active Brownian motion for which the particle self-propulsion is selected by a generalized velocity potential and fluctuates both in norm and direction. Considering the Fokker-Planck equation describing this fluctuating active dynamics, our analysis reveals that the expression of the nonequilibrium current in the hydrodynamic regime markedly depends on the details of the self-propulsion mechanism, while it satisfies the same symmetries as for constant-speed ABPs. Focusing on the case where the self-propulsion velocity derives from a quadratic potential, we moreover characterize the steady-state properties of the model in the presence of spatially varying activity. We find that density profiles created by activity landscapes

*benoit.mahault@ds.mpg.de

†ramin.golestanian@ds.mpg.de

are not only set by the mean particle self-propulsion speed, but also by its higher-order moments. We find that activity gradients generically correlate the particles' self-propulsion speed and orientation, and lead to an emergent polarization whose direction can point up or down the gradient depending on the model parameters. We discuss the consequences of the above features on the emergence of motility-induced phase separation [15]. Our work demonstrates that active fluctuations can be used as a way to control the spatial organization of active matter, and leads to conclusions in sharp contrast with the existing results obtained in the limit of constant-speed ABPs.

ABPs with active fluctuations. Contrary to thermal noise, the symmetries of active noise are dictated by that of the particle's self-propulsion velocity \mathbf{v} . Fluctuations of the norm $v \equiv |\mathbf{v}|$ and direction $\hat{\mathbf{n}} \equiv \mathbf{v}/v$ of the self-propulsion are thus generally decoupled. Therefore, we consider a model of overdamped ABPs in dimension $d \geq 2$ described by the following Langevin equations:

$$\dot{\mathbf{r}} = \mathbf{v} + \frac{1}{2}\nabla D_t(\mathbf{r}) + \sqrt{2D_t(\mathbf{r})}\xi_r(t), \quad (1a)$$

$$\dot{v} = -\partial_v W(\mathbf{r}, v) + \sqrt{2D_v(\mathbf{r})}\xi_v(t), \quad (1b)$$

$$\dot{\hat{\mathbf{n}}} = \sqrt{2D_r(\mathbf{r})}\mathbf{P}^\perp(\hat{\mathbf{n}}) \cdot \xi_r(t), \quad (1c)$$

where all model parameters may depend on the particle position \mathbf{r} while the unit variance, uncorrelated, Gaussian white noises ξ_r , ξ_v , and ξ_r , are interpreted in the Stratonovich sense. Equation (1a) describes the spatial dynamics of the particle with translational diffusivity $D_t(\mathbf{r})$. Moreover, it comprises a term compensating for the noise-induced drift that arises due to the multiplicative nature of the translational noise. The right-hand side of Eq. (1b) gathers two contributions. The first one corresponds to a deterministic active force that derives from an effective potential $W(\mathbf{r}, v)$, while the second contribution results from active fluctuations which are parameterized by the coefficient $D_v(\mathbf{r})$. Finally, Eq. (1c) sets the orientational dynamics of self-propulsion with associated diffusivity $D_r(\mathbf{r})$, where $P_{ij}^\perp(\hat{\mathbf{n}}) \equiv \delta_{ij} - \hat{n}_i\hat{n}_j$ denotes the projector orthogonal to $\hat{\mathbf{n}}$. Note that Eqs. (1b) and (1c) can equivalently be expressed in terms of the velocity \mathbf{v} . Keeping the Stratonovich interpretation of the noise, this leads to (see Supplemental Material [47])

$$\dot{\mathbf{v}} = -[\partial_v W + (d-1)\sqrt{D_v D_r}]\hat{\mathbf{n}} + \sqrt{2}\Sigma(\mathbf{v}) \cdot \xi(t),$$

with $\Sigma(\mathbf{v}) \equiv \sqrt{D_v}\hat{\mathbf{n}}\hat{\mathbf{n}} + v\sqrt{D_r}\mathbf{P}^\perp(\hat{\mathbf{n}})$. Therefore, due to the decoupling between the speed and orientational degrees of freedom, the noise on the self-propulsion velocity is generally multiplicative.

Denoting $\mathcal{P}(\mathbf{r}, v, \hat{\mathbf{n}}, t)$ as the single-particle distribution, it is straightforward to show that its dynamics follows

$$\partial_t \mathcal{P} = -\nabla \cdot \mathbf{J}_r - v^{1-d}\partial_v(v^{d-1}J_v) + D_r\nabla_{\hat{\mathbf{n}}}^2 \mathcal{P}, \quad (2)$$

where $\nabla_{\hat{\mathbf{n}}}^2 \equiv P_{ij}^\perp(\hat{\mathbf{n}})\partial_{\hat{n}_i}\partial_{\hat{n}_j} - (d-1)\hat{n}_i\partial_{\hat{n}_i}$ denotes the spherical Laplacian (summation over repeated indices is assumed), and the dependencies on \mathbf{r} , v , and $\hat{\mathbf{n}}$ are now implicit. The translational and speed currents are, respectively, given by $\mathbf{J}_r \equiv (\mathbf{v} - D_t\nabla)\mathcal{P}$ and $J_v \equiv -\partial_v W_{\text{eff}}\mathcal{P} - D_v\partial_v \mathcal{P}$, where the effective potential is defined as $W_{\text{eff}} \equiv W + (d-1)D_v \ln v$.

When the diffusivities and W are independent of \mathbf{r} , the steady-state solutions of Eq. (2) can be factorized and the speed distribution takes the Boltzmann-like form [44],

$$\mathcal{P}_H(v) = Z^{-1}e^{-W_{\text{eff}}(v)/D_v} = Z^{-1}v^{1-d}e^{-W(v)/D_v}, \quad (3)$$

with $Z \equiv \int_0^\infty dv e^{-W(v)/D_v}$ ensuring normalization.

Moment expansion. If the coefficients of Eq. (2) are spatially dependent, on the other hand, the active drift in \mathbf{J}_r coupling self-propulsion speed and orientation prevents any factorization of \mathcal{P} . However, the large-scale and long-time dynamics of the system is generally well captured by means of an expansion of Eq. (2) in the moments of \mathbf{v} . Given the symmetries of the problem, we shall not directly consider moments associated with \mathbf{v} , but rather those related to the corresponding speed v and orientation $\hat{\mathbf{n}}$. For the following discussion, we thus define the average: $\rho\langle \cdot \rangle \equiv \int v^{d-1}dv d\hat{\mathbf{n}}(\cdot)\mathcal{P}(\mathbf{r}, v, \hat{\mathbf{n}}, t)$, where $\rho(\mathbf{r}, t) = \rho(1)$ is the local particle density normalized to unity. Deriving the equations for the moments (details in Appendix A), we find that the nature and number of terms they involve closely depend on the specific form of W . It is, moreover, clear that the unique slow mode of the dynamics is the conserved particle density ρ , which satisfies $\partial_t \rho = -\nabla \cdot \mathbf{J}$ with $\mathbf{J} = \rho\langle v\hat{\mathbf{n}} \rangle - D_t\nabla\rho$. Therefore, in the long-time and large-scale limit, the dynamics of all higher-order, i.e., in speed and orientations, moments can be enslaved to ρ .

In order to keep the presentation simple while retaining relevant features of active fluctuations, we consider the quadratic form $W(\mathbf{r}, v) = \frac{\mu(\mathbf{r})}{2}[v - v_0(\mathbf{r})]^2$, where μ and v_0 are a function of space and assumed positive. With this choice of the potential, the velocity dynamics has four parameters which can all be experimentally evaluated from individual particle tracking. $\tau_r \equiv [(d-1)D_r]^{-1}$ sets the typical timescale of rotational diffusion, while μ^{-1} controls the speed relaxation. Assuming a homogeneous system, both can be measured from the steady-state autocorrelation of the particle self-propulsion direction and speed. Namely, $\langle \hat{\mathbf{n}}(t) \cdot \hat{\mathbf{n}}(t + \tau) \rangle = e^{-\tau/\tau_r}$ and $\langle v(t)v(t + \tau) \rangle = \langle v^2 \rangle e^{-\mu\tau}$. Moreover, v_0 and D_v can be obtained from the full speed distribution (3) or simply from its first two moments:

$$\langle v \rangle_H = v_0 + \frac{D_v}{\mu}\gamma, \quad \langle v^2 \rangle_H = \frac{D_v}{\mu} + v_0\langle v \rangle_H, \quad (4)$$

where the subscript H refers to averages computed with the distribution (3), while $\gamma = \sqrt{2\mu/(D_v\pi)}f(\mu v_0^2/D_v)$ and $f(x) \equiv e^{-x/2}/[1 + \text{Erf}(\sqrt{x/2})]$. We note that the limit of constant-speed ABPs is recovered for $\mu \rightarrow \infty$, such that $\langle v \rangle_H$ instantly relaxes to v_0 . On the other hand, taking D_v and μ finite with $v_0 = 0$ amounts to a variant of the active Ornstein-Uhlenbeck particles [48], where speed and orientation fluctuations are decoupled.

We show in Appendix A that for up to $O(\nabla^2)$ terms, the self-propulsion speed moments are given by $\langle v^k \rangle = \langle v^k \rangle_H$, where $\mathcal{P}_H(\mathbf{r}, v)$ now varies in space as a result of the spatial dependencies of W and D_v . Similarly, we find that at this order in gradients, the polarity moments can be expressed in terms of $\nabla(\rho\langle v^k \rangle)$ with $k \geq 1$. Replacing the relevant expressions into the particle density current, we finally obtain, in the

hydrodynamic limit,

$$\mathbf{J} = -D_t \nabla \rho - \frac{\tau_r}{d(1+\alpha)} [\nabla(\rho \langle v^2 \rangle) + \alpha v_0 \nabla(\rho \langle v \rangle)], \quad (5)$$

where $\alpha \equiv \mu \tau_r$. For a quadratic potential W , the density dynamics is therefore uniquely determined by the first two self-propulsion speed moments. For $v_0 > 0$ and a fast active speed dynamics ($\alpha \gg 1$), the dependency of \mathbf{J} in $\langle v^2 \rangle$ also drops out so that its expression reduces to that of constant-speed ABPs [49]. Below, we discuss the consequences of finite- α values on the steady-state density. We also present parameter-free comparisons of our results with simulations of the Langevin system (1) in three dimensions; see the Supplemental Material [47] for more details about the numerical methods.

Inhomogeneous steady states. For flux-free boundary conditions, the stationary density profile $\rho_s(\mathbf{r})$ is simply obtained from the condition $\mathbf{J} = \mathbf{0}$, leading to

$$\nabla \ln \rho_s = - \frac{\nabla \langle v^2 \rangle + \alpha v_0 \nabla \langle v \rangle}{v_D^2 (1+\alpha) + \langle v^2 \rangle + \alpha v_0 \langle v \rangle}, \quad (6)$$

where we have defined $v_D \equiv (d D_t \tau_r^{-1})^{1/2}$ as the velocity scale built from the translational and rotational diffusivities. Equation (6) predicts that spatially varying activity resulting in nonvanishing gradients of the self-propulsion speed moments leads to inhomogeneous density profiles. From the expressions of the moments in Eq. (4), particle segregation can thus be achieved independently by imposing gradients of v_0 , D_v , or μ . Conversely, the translational diffusion coefficient only appears in Eq. (6) through v_D , so that its spatial variations will not qualitatively affect ρ_s . For simplicity, we thus neglect its contribution for the remainder of this discussion.

Setting $v_D = 0$, the rotational diffusivity D_r appears in the expression of ρ_s only through the parameter α . Spatial variations of D_r alone are therefore unable to generate density gradients, in agreement with usual considerations [15] and recent experimental results [50]. However, the value of α sets the scaling of the steady-state density with the speed moments. For fast speed dynamics ($\alpha \gg 1$), Eq. (6) leads to the standard relation $\rho_s \sim \langle v \rangle^{-1}$ [49], while in the opposite case of fast rotational diffusion ($\alpha \ll 1$), we instead get $\rho_s \sim \langle v^2 \rangle^{-1}$. Assuming α to be uniform, we moreover obtain from Eq. (6) in the active force, or noise dominated, the regimes

$$\rho_s \sim v_0^{-(2+\alpha)/(1+\alpha)} \quad (D_v \ll \mu v_0^2), \quad (7a)$$

$$\rho_s \sim \langle v \rangle^{-2} \sim (D_v/\mu)^{-1} \quad (D_v \gg \mu v_0^2). \quad (7b)$$

For low noises, the steady-state density therefore scales algebraically with the mean particle speed, with an exponent set by the ratio between the rotational diffusion and speed relaxation timescales, as shown in Fig. 1(a). On the contrary, when active noise dominates, Fig. 1(b) shows that the effect of rotational noise disappears, as ρ_s always scales as the inverse of D_v/μ .

From Eq. (6), for D_v and μv_0^2 of similar order, the stationary density is no more enslaved to the mean particle speed, as gradients of $\langle v^2 \rangle$ can compete with that of $\langle v \rangle$. This feature allows for counterintuitive behavior, as we show by considering the following illustrative setup: we partition the space into two distinct subregions 1 and 2 in which active particles experience different uniform values of $v_0 = v_{1,2}$ and $D_v = D_{v,2}$

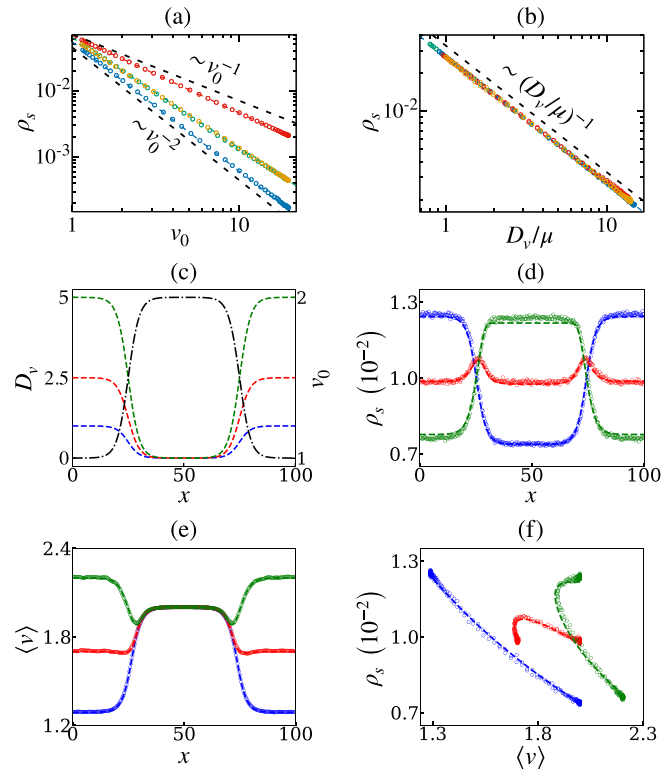


FIG. 1. Steady-state density with spatially varying activity. (a) Mean stationary density as a function of v_0 for $\mu v_0^2 \gg D_v$; the colors, respectively, correspond to $(\mu, D_r) = (1, 1)$ (green), $(1, 10)$ (blue), $(10, 1)$ (red), and $(10, 10)$ (yellow). (b) Mean stationary density as a function of D_v/μ for $\mu v_0^2 \ll D_v$; the color code is the same as (a). In (a) and (b), the data have been shifted vertically for clarity. (c) Imposed one-dimensional v_0 (black dash-dotted line) and D_v (colored dashed lines) profiles splitting the space in two nearly homogeneous regions with different activities. (d), (e) The (d) mean density and (e) particle speed profiles corresponding to (c). (f) The relation $\rho(\langle v \rangle)$ corresponding to (d) and (e). In (d)–(f), $\mu = D_r = 1$, the $v_0(x)$ profile is unchanged, and the color codes the maximal value of D_v in each case. In all panels except (c), open circles show the results obtained from Langevin simulations, while dashed lines indicate the corresponding theoretical predictions.

[see Fig. 1(c)]. We denote $\tilde{v} = v_1 - v_2$ and $\tilde{D}_v = D_{v_1} - D_{v_2}$, and consider the case $\tilde{v} \tilde{D}_v < 0$. \tilde{v} is kept fixed and we vary \tilde{D}_v . For sufficiently small $|\tilde{D}_v|$, ρ_s is maximal in the region with the smallest v_0 , as is generally the case for constant-speed ABPs [15, 49] [see blue lines in Figs. 1(c) and 1(d)]. Increasing $|\tilde{D}_v|$ progressively leads to an inversion of the density profile, such that for large $|\tilde{D}_v|$, particles instead accumulate, on average, in the region where v_0 is largest [green lines in Figs. 1(c) and 1(d)]. The density inversion partly follows the behavior of the mean speed $\langle v \rangle$, also affected by $|\tilde{D}_v|$ [see Eq. (4) and Fig. 1(e)]. While ρ_s globally remains largest in small $\langle v \rangle$ regions, a direct inspection of the $\rho_s(\langle v \rangle)$ curves reveals that when ∇v_0 and ∇D_v are both nonzero, ρ_s can locally increase with $\langle v \rangle$ [Fig. 1(f)], which is something that is impossible in the absence of active fluctuations.

Orientation-speed correlations and emergent polarization. The phase-space distribution solving Eq. (2) with spatially

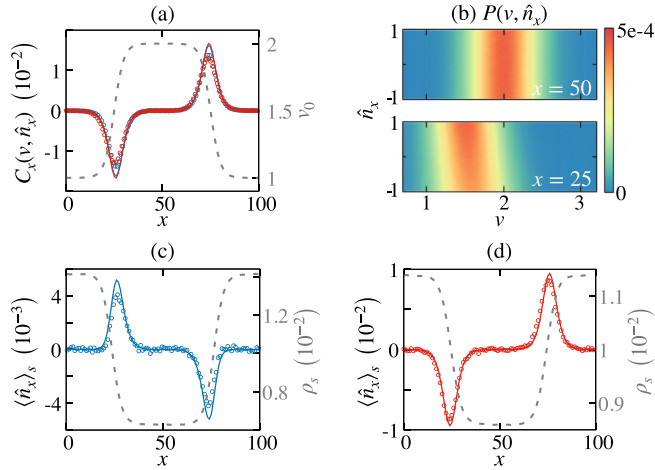


FIG. 2. Speed-order correlations and local polarization. (a) The steady-state correlation function $C_x(v, \hat{n}_x)$ in the presence of spatially varying activity $v_0(x)$ (gray dashed lines) as well as uniform $D_v = 0.1$ and $\mu = D_r = 1$ with $D_r = 0.1$ (blue) and 1 (red). (b) The joint speed-orientation distribution associated with (a) for $D_r = 0.1$, at the center of the domain ($x = 50$) and at the interface between the two regions with different activities ($x = 25$). (c),(d) The local averaged polarization profiles corresponding to (a) with the same color code, while the dashed gray line shows the corresponding stationary density profiles. In (a), (c), and (d), open circles show the simulations data, while continuous lines indicate theoretical predictions.

varying coefficients cannot be factorized due to the coupling between the particle motion and activity [Fig. 2(b)]. We now discuss the consequences of such feature on the particles' orientational dynamics in the presence of activity landscapes. In order to avoid dealing with lengthy expressions, we focus on the limiting case $\mu v_0^2 \gg D_v$, but the results presented below hold in a more general context. General expressions are presented in the Supplemental Material [47].

Correlations between the speed and the orientation of the active particles are quantified considering the connected moment $\mathbf{C}(v, \hat{n}) \equiv \langle v \hat{n} \rangle - \langle v \rangle \langle \hat{n} \rangle$, for which we find

$$\mathbf{C}(v, \hat{n}) = -\frac{\tau_r v_0 \nabla v_0}{d(1 + \alpha)} \quad (\mu v_0^2 \gg D_v), \quad (8)$$

showing that \mathbf{C} is nonzero in regions of nonvanishing activity gradients, as illustrated in Fig. 2(a). Naturally, speed-orientation correlations are also suppressed in the cases of fast rotational and speed relaxation, respectively, for $\tau_r \rightarrow 0$ and $\alpha \gg 1$.

Moreover, spatially varying activity spontaneously generates local orientational order. Namely, using the zero flux solution (6) and the expression of the polarization given in Appendix A, we find, in the stationary state,

$$\langle \hat{n} \rangle_s = \frac{\tau_r}{d} \frac{v_0^2 - v_D^2(1 + \alpha)}{(1 + \alpha)(v_D^2 + v_0^2)} \nabla v_0 \quad (\mu v_0^2 \gg D_v). \quad (9)$$

Equation (9) highlights two mechanisms at the origin of the polar order in regions of nonzero activity gradients. For fast speed relaxation ($\alpha \gg 1$), the steady-state active flux $\langle v \hat{n} \rangle_s \sim v_0 \langle \hat{n} \rangle_s$ must compensate the diffusive flux $-D_t \nabla \rho_s$ so that $\langle \hat{n} \rangle_s$ points towards slow (or dense)

regions [see Fig. 2(d)] [23,51,52]. This gradient alignment mechanism is consistent with the polarization generally observed at interfaces of repelling ABPs in the phase-separated regime [53–55], where, in this case, the mean-field spatial diffusion results from particle collisions [56]. On the other hand, for self-propulsion speeds v_0 such that $v_0^2 > v_D^2(1 + \alpha)$, Eq. (9) predicts a reversal of the mean polarization direction towards fast (or dilute) regions [see Fig. 2(c)]. Indeed, neglecting the effect of positional diffusion particles crossing an interface separating two regions with different activities will be, on average, slower—and thus stay longer at the interface—if they come from the slower (or denser) region. Consequently, the local polarization will, in this case, be oriented towards the most dilute region.

Motility-induced phase separation (MIPS). The origin of MIPS can be understood at the mean-field level from a mapping to a dynamics with quorum-sensing interactions, where the particles' motility effectively depends on their local density [15,56]. In the case where active particles slow down sufficiently fast as they reach denser regions, homogeneous systems may indeed undergo an instability which marks the onset of phase separation. As the above derivation considers general spatial dependencies of the model parameters, it allows us to study how active fluctuations can trigger or influence the onset of MIPS. Here, we assume ρ to be sufficiently large such that its fluctuations can be neglected [57]. Consequently, we consider Eq. (5) with all coefficients being functions of $\varrho \equiv \int d^d \mathbf{r}' K(|\mathbf{r} - \mathbf{r}'|) \rho(\mathbf{r}')$, where K is a (normalized) short-range interaction kernel. Expanding ϱ in the gradients of ρ , the active noise dynamics with quorum-sensing interactions maps to active model B (AMB) [58], such that the current in (5) can be formally written as $\mathbf{J} = -\rho M(\varrho) \nabla \psi(\rho)$, where the generalized chemical potential is given by $\psi(\rho) = f'(\rho) - \kappa(\rho) \nabla^2 \rho$. The expressions of the coefficients $f'(\rho)$ and $\kappa(\rho)$, as well as details on the derivation, are given in Appendix B.

We deduce that a homogeneous system at density $\bar{\rho}$ is linearly unstable to small wave-number perturbations whenever $f''(\bar{\rho}) < 0$. In the limiting cases of large active force and noise, we find that this condition translates to

$$\frac{v_0'(2 + \alpha)}{v_0(1 + \alpha)} \frac{\bar{\rho}}{1 + \frac{v_D^2}{v_0^2}} < -1 \quad (D_v \ll \mu v_0^2), \quad (10a)$$

$$\frac{(D_v/\mu)'}{D_v/\mu} \frac{\bar{\rho}}{1 + (1 + \alpha) \frac{v_D^2 \mu}{D_v}} < -1 \quad (D_v \gg \mu v_0^2), \quad (10b)$$

where dependencies of the coefficients in ρ are implicit to lighten the notation, and prime denotes differentiation with respect to ρ . We observe from Eq. (10b) that in addition to the standard route, MIPS may also be caused by active fluctuations, as well as cases where the speed-relaxation timescale μ^{-1} depends on the local density. Moreover, since the instability condition can be fulfilled only if $\langle v \rangle$ or $\langle v^2 \rangle$ depend on ρ (see Appendix B), $D_r(\rho)$ by itself cannot lead to MIPS, but will affect the determination of the spinodals in a nontrivial way through the coefficient α . Indeed, taking Eq. (10a) with $v_D = 0$, the instability condition becomes $\bar{\rho} v_0'/v_0 < -(1 + \alpha)/(2 + \alpha)$. For $\alpha \gg 1$, this condition reduces to that of constant-speed ABPs [15,57], but smaller values of α , in turn,

lead to a less strict condition such that spinodal decomposition may be observed even if $\bar{\rho}v'_0/v_0 > -1$. Finally, when the full dependency of the model parameters on the local particle density is known, the MIPS binodals can be computed from $\psi(\rho)$ using the mapping to generalized thermodynamic variables outlined in Ref. [54].

We have introduced a general model of active noise and studied its consequences on the free motion of ABPs. Our analysis reveals a number of quantitative differences with respect to the widely used constant-speed ABPs model, such as the breakdown of the $\rho_s \sim \langle v \rangle^{-1}$ law for comparable self-propulsion speed and orientational relaxation timescales, leading under these conditions to possibly counterintuitive stationary density profiles in activity landscapes. Moreover, our results illustrate how the interplay of active noise and activity gradients leads to correlations between particles speeds and orientation, as well as emergent polar order in the absence of explicit aligning interactions. Considering a system with quorum-sensing interactions, we have shown how active noise modifies the MIPS phase diagram. In particular, our results suggest that active fluctuations could constitute a mechanistic explanation of the motility-induced clustering phenomena observed in systems for which the MIPS instability condition for constant-speed ABPs does not hold [39]. Considering more complex expressions of the potential W or other types of particle interactions [59,60], it thus appears clear that further consequences of active noise on the dynamics of active matter are expected.

Acknowledgments. This work has received support from the Max Planck School Matter to Life and the MaxSynBio Consortium, which are jointly funded by the Federal Ministry of Education and Research (BMBF) of Germany, and the Max Planck Society.

APPENDIX A: THE DERIVATION OF EQ. (5)

Here, we provide technical details on the moment expansion and closure procedure leading to the hydrodynamic current (5) for the density field ρ .

Using the definition $\rho(\cdot) = \int v^{d-1} dv d\hat{n}(\cdot) \mathcal{P}(\mathbf{r}, v, \hat{n}, t)$ of the velocity moments, after some algebra we obtain, from Eq. (2) and for $k \geq 0$,

$$\partial_t(\rho\langle v^k \rangle) = -\nabla \cdot [\rho\langle \hat{n}v^{k+1} \rangle - D_t \nabla(\rho\langle v^k \rangle)] + \rho\langle \mathcal{G}_k \rangle + b_k, \quad (\text{A1a})$$

$$\partial_t(\rho\langle \hat{n}v^k \rangle) = -\nabla \cdot \left[\rho\langle \mathbf{q}v^{k+1} \rangle + \frac{\mathbf{I}}{d}\rho\langle v^{k+1} \rangle - D_t \nabla(\rho\langle \hat{n}v^k \rangle) \right] - (d-1)D_r \rho\langle \hat{n}v^k \rangle + \rho\langle \hat{n}\mathcal{G}_k \rangle + \nabla\phi_k, \quad (\text{A1b})$$

where $\mathbf{q} \equiv \hat{n}\hat{n} - \mathbf{I}/d$ measures nematic order, and $\mathcal{G}_k \equiv k[(k-1)v^{k-2}D_v - v^{k-1}\partial_v W]$. The boundary terms b_k and $\nabla\phi_k$ on the right-hand side of Eqs. (A1) are obtained after integrating by parts the speed current in Eq. (2); their presence results from the singular behavior of \mathcal{P} at $v=0$ [see Eq. (3)].

Namely, they are given by

$$b_k = \lim_{v \rightarrow 0} \int d\hat{n} v^{k+d-1} \left[\frac{kD_v}{v} - \partial_v W_{\text{eff}} - D_v \partial_v \right] \mathcal{P},$$

$$\nabla\phi_k = \lim_{v \rightarrow 0} \int d\hat{n} \hat{n} v^{k+d-1} \left[\frac{kD_v}{v} - \partial_v W_{\text{eff}} - D_v \partial_v \right] \mathcal{P}.$$

To evaluate them, we show in the Supplemental Material [47] that the distribution $\mathcal{P}(\mathbf{r}, v, \hat{n}, t)$ can be written perturbatively as

$$\mathcal{P}(\mathbf{r}, v, \hat{n}, t) \simeq \rho(\mathbf{r}, t) \frac{\mathcal{P}_H(\mathbf{r}, v)}{\mathcal{S}_d} [1 + Y(\mathbf{r}, v, \hat{n})],$$

where \mathcal{S}_d denotes the surface of the unit $(d-1)$ -sphere, \mathcal{P}_H is given by (3) with space-dependent W and D_v , while the $O(\hat{n} \cdot \nabla)$ function Y is unknown but satisfies in the regime $D_v \gg W$ relevant for the boundary terms:

$$Y(\mathbf{r}, v, \hat{n}) \underset{D_v \gg W}{\simeq} -v\tau_r(\hat{n} \cdot \nabla) \ln[\mathcal{P}_H(\mathbf{r}, v)].$$

Using these expressions, we therefore obtain

$$b_k = D_v \rho \gamma \delta_{k,1}, \quad \nabla\phi_k = \frac{D_v \tau_r \delta_{k,0}}{d} \nabla(\rho\gamma), \quad (\text{A2})$$

where $\gamma(\mathbf{r}) \equiv \mathcal{P}_H(\mathbf{r}, 0) = e^{-W(\mathbf{r}, 0)/D_v(\mathbf{r})} Z^{-1}(\mathbf{r})$ and $\delta_{i,j}$ is the Kronecker delta symbol.

Considering now $W(\mathbf{r}, v) = \frac{\mu(r)}{2}[v - v_0(\mathbf{r})]^2$, we express from Eq. (A1b) the first two polarity moments as

$$\rho\langle \hat{n} \rangle = -\frac{\tau_r}{d} \nabla(\rho\langle v \rangle) + \frac{D_v \tau_r^2}{d} \nabla(\rho\gamma), \quad (\text{A3a})$$

$$\rho\langle v\hat{n} \rangle = -\frac{\tau_r}{d(1+\alpha)} \nabla(\rho\langle v^2 \rangle) + \frac{\alpha v_0}{1+\alpha} \rho\langle \hat{n} \rangle, \quad (\text{A3b})$$

where $\alpha \equiv \mu\tau_r$ and we have kept only contributions up to $O(\nabla)$. In particular, the contribution from the nematic order parameter \mathbf{q} was discarded as it is $O(\nabla^2)$ (see Supplemental Material [47]). At first order in gradients, the self-propulsion speed moments moreover solve $\langle \mathcal{G}_k \rangle + b_k = 0$, such that $\langle v^k \rangle = \langle v^k \rangle_H$, where the H subscript indicates that the average is taken with respect to the distribution $\mathcal{P}_H(\mathbf{r}, v)$. Noting that the density satisfies, from (A1a) with $k=0$,

$$\partial_t \rho = -\nabla \cdot [\rho\langle v\hat{n} \rangle - D_t \nabla \rho],$$

and combining Eqs. (4) and (A3), finally gives the hydrodynamic current (5). Note that the boundary term $\sim \tau_r^2 D_v v_0 \nabla(\rho\gamma)$ coming from (A3a) has been discarded as its contribution is generally subleading.

APPENDIX B: THE MAPPING TO AMB

Here, we present the derivation of the nonlocal currents arising when the interactions between the particles can be treated as effective quorum-sensing interactions, leading to a dependence in the particle density of the hydrodynamic equation coefficients. Let us therefore consider the hydrodynamic current (5) and assume that all coefficients take a functional dependency in the local density field such that

$$\langle v^2 \rangle(\varrho), \langle v \rangle(\varrho), v_0(\varrho), \tau_r(\varrho), \alpha(\varrho), D_t(\varrho), \quad (\text{B1})$$

where $\varrho \equiv \int d^d \mathbf{r}' K(|\mathbf{r}' - \mathbf{r}|) \rho(\mathbf{r}')$ and K is a short-range interaction kernel normalized such that $\int d^d \mathbf{r}' K(\mathbf{r}') = 1$. We

now define

$$M(\varrho) \equiv D_t(\varrho) + \frac{\tau_r(\varrho)}{d[1 + \alpha(\varrho)]} [\langle v^2 \rangle(\varrho) + \alpha(\varrho)v_0(\varrho)\langle v \rangle(\varrho)] \quad (\text{B2})$$

as an effective mobility for the dynamics. Note that this choice is arbitrary as long as $M(\varrho) > 0$. The current in Eq. (5) is then written as

$$\mathbf{J} = -\rho M(\varrho) \left[\nabla \ln(\rho) + \frac{\nabla[\langle v^2 \rangle(\varrho)] + \alpha(\varrho)v_0(\varrho)\nabla[\langle v \rangle(\varrho)]}{[1 + \alpha(\varrho)]v_D^2(\varrho) + \langle v^2 \rangle(\varrho) + \alpha(\varrho)v_0(\varrho)\langle v \rangle(\varrho)} \right],$$

where $v_D^2 \equiv dD_t\tau_r^{-1}$. Assuming that ρ does not vary much over the scale of the quorum-sensing interaction, we expand for any function $\phi(\varrho)$ up to second order in gradient:

$$\phi(\varrho) \simeq \phi(\rho + \ell^2 \nabla^2 \rho) \simeq \phi(\rho) + \ell^2 \phi'(\rho) \nabla^2 \rho,$$

where $\ell^2 \equiv \frac{1}{2d} \int d^d \mathbf{r} K(r)r^2$ and prime denotes the derivative with respect to ρ . Expanding all coefficients in the fraction on the right-hand side of (B3), we find after some algebra that the current can be recast into the compact form $\mathbf{J} = -\rho M(\varrho) \nabla \psi(\rho)$, where the effective chemical potential $\psi(\rho) \equiv f'(\rho) - \kappa(\rho) \nabla^2 \rho$, while the generalized free energy and surface tension are defined as

$$f'(\rho) \equiv \ln(\rho) + \int^\rho dy \frac{\langle v^2 \rangle' + \alpha v_0 \langle v \rangle'}{(1 + \alpha)v_D^2 + \langle v^2 \rangle + \alpha v_0 \langle v \rangle},$$

$$\kappa(\rho) \equiv -\ell^2 \frac{\langle v^2 \rangle' + \alpha v_0 \langle v \rangle'}{(1 + \alpha)v_D^2 + \langle v^2 \rangle + \alpha v_0 \langle v \rangle},$$

where the ρ dependency of the coefficients is kept implicit to lighten notations.

-
- [1] J. Prost, F. Jülicher, and J.-F. Joanny, Active gel physics, *Nat. Phys.* **11**, 111 (2015).
- [2] A. Doostmohammadi, J. Ignés-Mullol, J. M. Yeomans, and F. Sagués, Active nematics, *Nat. Commun.* **9**, 3246 (2018).
- [3] R. Golestanian, Phoretic active matter, *Active Matter and Nonequilibrium Statistical Physics: Lecture Notes of the Les Houches Summer School: Vol. 112* (Oxford University Press, Oxford, 2022), <https://doi.org/10.1093/oso/9780192858313.001.0001>.
- [4] R. Soto and R. Golestanian, Self-Assembly of Catalytically Active Colloidal Molecules: Tailoring Activity Through Surface Chemistry, *Phys. Rev. Lett.* **112**, 068301 (2014).
- [5] S. Saha, S. Ramaswamy, and R. Golestanian, Pairing, waltzing and scattering of chemotactic active colloids, *New J. Phys.* **21**, 063006 (2019).
- [6] S. Saha, J. Agudo-Canalejo, and R. Golestanian, Scalar Active Mixtures: The Nonreciprocal Cahn-Hilliard Model, *Phys. Rev. X* **10**, 041009 (2020).
- [7] Z. You, A. Baskaran, and M. C. Marchetti, Nonreciprocity as a generic route to traveling states, *Proc. Natl. Acad. Sci. USA* **117**, 19767 (2020).
- [8] L. P. Dadhichi, J. Kethapelli, R. Chajwa, S. Ramaswamy, and A. Maitra, Nonmutual torques and the unimportance of motility for long-range order in two-dimensional flocks, *Phys. Rev. E* **101**, 052601 (2020).
- [9] M. Fruchart, R. Hanai, P. B. Littlewood, and V. Vitelli, Non-reciprocal phase transitions, *Nature (London)* **592**, 363 (2021).
- [10] D. Dell'Arciprete, M. L. Blow, A. T. Brown, F. D. C. Farrell, J. S. Lintuvuori, A. F. McVey, D. Marenduzzo, and W. C. K. Poon, A growing bacterial colony in two dimensions as an active nematic, *Nat. Commun.* **9**, 4190 (2018).
- [11] Z. You, D. J. G. Pearce, A. Sengupta, and L. Giomi, Geometry and Mechanics of Microdomains in Growing Bacterial Colonies, *Phys. Rev. X* **8**, 031065 (2018).
- [12] R. Hartmann, P. K. Singh, P. Pearce, R. Mok, B. Song, F. Díaz-Pascual, J. Dunkel, and K. Drescher, Emergence of three-dimensional order and structure in growing biofilms, *Nat. Phys.* **15**, 251 (2019).
- [13] P. Romanczuk, M. Bär, W. Ebeling, B. Lindner, and L. Schimansky-Geier, Active Brownian particles, *Eur. Phys. J.: Spec. Top.* **202**, 1 (2012).
- [14] M. C. Marchetti, J. F. Joanny, S. Ramaswamy, T. B. Liverpool, J. Prost, M. Rao, and R. A. Simha, Hydrodynamics of soft active matter, *Rev. Mod. Phys.* **85**, 1143 (2013).
- [15] M. E. Cates and J. Tailleur, Motility-induced phase separation, *Annu. Rev. Condens. Matter Phys.* **6**, 219 (2015).
- [16] G. Gompper *et al.*, The 2020 motile active matter road map, *J. Phys.: Condens. Matter* **32**, 193001 (2020).
- [17] H. Chaté, Dry aligning dilute active matter, *Annu. Rev. Condens. Matter Phys.* **11**, 189 (2020).
- [18] W. Gao and J. Wang, The environmental impact of micro/nanomachines: A review, *ACS Nano* **8**, 3170 (2014).
- [19] A. Ghosh, W. Xu, N. Gupta, and D. H. Gracias, Active matter therapeutics, *Nano Today* **31**, 100836 (2020).
- [20] C. Lozano, B. ten Hagen, H. Löwen, and C. Bechinger, Phototaxis of synthetic microswimmers in optical landscapes, *Nat. Commun.* **7**, 12828 (2016).
- [21] J. Arlt, V. A. Martinez, A. Dawson, T. Pilizota, and W. C. K. Poon, Painting with light-powered bacteria, *Nat. Commun.* **9**, 768 (2018).
- [22] G. Frangipane, D. Dell'Arciprete, S. Petracchini, C. Maggi, F. Saglimbeni, S. Bianchi, G. Vizsnyiczai, M. L. Bernardini, and R. Di Leonardo, Dynamic density shaping of photokinetic *E. coli*, *Elife* **7**, e36608 (2018).
- [23] N. A. Söker, S. Auschra, V. Holubec, K. Kroy, and F. Cichos, How Activity Landscapes Polarize Microswimmers without Alignment Forces, *Phys. Rev. Lett.* **126**, 228001 (2021).
- [24] T. Bäuerle, A. Fischer, T. Speck, and C. Bechinger, Self-organization of active particles by quorum sensing rules, *Nat. Commun.* **9**, 3232 (2018).
- [25] F. A. Lavergne, H. Wendehenne, T. Bäuerle, and C. Bechinger, Group formation and cohesion of active particles with visual perception-dependent motility, *Science* **364**, 70 (2019).
- [26] A. I. Curatolo, N. Zhou, Y. Zhao, C. Liu, A. Daerr, J. Tailleur, and J. Huang, Cooperative pattern formation in multicomponent bacterial systems through reciprocal motility regulation, *Nat. Phys.* **16**, 1152 (2020).

- [27] J. Elgeti, R. G. Winkler, and G. Gompper, Physics of microswimmers—Single particle motion and collective behavior: A review, *Rep. Prog. Phys.* **78**, 056601 (2015).
- [28] R. Golestanian, Anomalous Diffusion of Symmetric and Asymmetric Active Colloids, *Phys. Rev. Lett.* **102**, 188305 (2009).
- [29] C. Bechinger, R. Di Leonardo, H. Löwen, C. Reichhardt, G. Volpe, and G. Volpe, Active particles in complex and crowded environments, *Rev. Mod. Phys.* **88**, 045006 (2016).
- [30] H. C. Berg and D. A. Brown, Chemotaxis in *Escherichia coli* analysed by three-dimensional tracking, *Nature (London)* **239**, 500 (1972).
- [31] Y. Magariyama, S. Sugiyama, K. Muramoto, I. Kawagishi, Y. Imae, and S. Kudo, Simultaneous measurement of bacterial flagellar rotation rate and swimming speed, *Biophys. J.* **69**, 2154 (1995).
- [32] W. F. Paxton, K. C. Kistler, C. C. Olmeda, A. Sen, S. K. St. Angelo, Y. Cao, T. E. Mallouk, P. E. Lammert, and V. H. Crespi, Catalytic Nanomotors: Autonomous Movement of Striped Nanorods, *J. Am. Chem. Soc.* **126**, 13424 (2004).
- [33] R. Dreyfus, J. Baudry, M. L. Roper, M. Fermigier, H. A. Stone, and J. Bibette, Microscopic artificial swimmers, *Nature (London)* **437**, 862 (2005).
- [34] J. R. Howse, R. A. L. Jones, A. J. Ryan, T. Gough, R. Vafabakhsh, and R. Golestanian, Self-Motile Colloidal Particles: From Directed Propulsion to Random Walk, *Phys. Rev. Lett.* **99**, 048102 (2007).
- [35] G. Corkidi, B. Taboada, C. Wood, A. Guerrero, and A. Darszon, Tracking sperm in three-dimensions, *Biochem. Biophys. Res. Commun.* **373**, 125 (2008).
- [36] S. Thutupalli, R. Seemann, and S. Herminghaus, Swarming behavior of simple model squirmers, *New J. Phys.* **13**, 073021 (2011).
- [37] G. Grosjean, M. Hubert, G. Lagubeau, and N. Vandewalle, Realization of the Najafi-Golestanian microswimmer, *Phys. Rev. E* **94**, 021101(R) (2016).
- [38] L. Turner, L. Ping, M. Neubauer, and H. C. Berg, Visualizing flagella while tracking bacteria, *Biophys. J.* **111**, 630 (2016).
- [39] A. A. Fragkopoulos, J. Vachier, J. Frey, F.-M. Le Menn, M. G. Mazza, M. Wilczek, D. Zwicker, and O. Bäümchen, Self-generated oxygen gradients control collective aggregation of photosynthetic microbes, *J. R. Soc. Interface* **18**, 20210553 (2021).
- [40] R. Golestanian, T. B. Liverpool, and A. Ajdari, Propulsion of a Molecular Machine by Asymmetric Distribution of Reaction Products, *Phys. Rev. Lett.* **94**, 220801 (2005).
- [41] A. Najafi and R. Golestanian, Simple swimmer at low Reynolds number: Three linked spheres, *Phys. Rev. E* **69**, 062901 (2004).
- [42] M. Schienbein and H. Gruler, Langevin equation, Fokker-Planck equation and cell migration, *Bull. Math. Biol.* **55**, 585 (1993).
- [43] F. Peruani and L. G. Morelli, Self-Propelled Particles with Fluctuating Speed and Direction of Motion in Two Dimensions, *Phys. Rev. Lett.* **99**, 010602 (2007).
- [44] P. Romanczuk and L. Schimansky-Geier, Brownian Motion with Active Fluctuations, *Phys. Rev. Lett.* **106**, 230601 (2011).
- [45] D. Chaudhuri, Active Brownian particles: Entropy production and fluctuation response, *Phys. Rev. E* **90**, 022131 (2014).
- [46] L. Caprini, A. R. Sprenger, H. Löwen, and R. Wittmann, The parental active model: A unifying stochastic description of self-propulsion, *J. Chem. Phys.* **156**, 071102 (2022).
- [47] See Supplemental Material at <http://link.aps.org/supplemental/10.1103/PhysRevResearch.5.L022012> for additional details about the moment expansion and derivations of the orientational moments, as well as technical details about numerical simulations of the Langevin equations.
- [48] D. Martin, J. O’Byrne, M. E. Cates, E. Fodor, C. Nardini, J. Tailleur, and F. van Wijland, Statistical mechanics of active Ornstein-Uhlenbeck particles, *Phys. Rev. E* **103**, 032607 (2021).
- [49] M. J. Schnitzer, Theory of continuum random walks and application to chemotaxis, *Phys. Rev. E* **48**, 2553 (1993).
- [50] M. A. Fernandez-Rodriguez, F. Grillo, L. Alvarez, M. Rathlef, I. Buttinoni, G. Volpe, and L. Isa, Feedback-controlled active Brownian colloids with space-dependent rotational dynamics, *Nat. Commun.* **11**, 4223 (2020).
- [51] A. Fischer, F. Schmid, and T. Speck, Quorum-sensing active particles with discontinuous motility, *Phys. Rev. E* **101**, 012601 (2020).
- [52] H. Row and J. F. Brady, Reverse osmotic effect in active matter, *Phys. Rev. E* **101**, 062604 (2020).
- [53] C. F. Lee, Interface stability, interface fluctuations, and the Gibbs-Thomson relationship in motility-induced phase separations, *Soft Matter* **13**, 376 (2017).
- [54] A. P. Solon, J. Stenhammar, M. E. Cates, Y. Kafri, and J. Tailleur, Generalized thermodynamics of motility-induced phase separation: Phase equilibria, Laplace pressure, and change of ensembles, *New J. Phys.* **20**, 075001 (2018).
- [55] A. K. Omar, Z.-G. Wang, and J. F. Brady, Microscopic origins of the swim pressure and the anomalous surface tension of active matter, *Phys. Rev. E* **101**, 012604 (2020).
- [56] J. Bialké, H. Löwen, and T. Speck, Microscopic theory for the phase separation of self-propelled repulsive disks, *Europhys. Lett.* **103**, 30008 (2013).
- [57] A. P. Solon, M. E. Cates, and J. Tailleur, Active Brownian particles and run-and-tumble particles: A comparative study, *Eur. Phys. J.: Spec. Top.* **224**, 1231 (2015).
- [58] R. Wittkowski, A. Tiribocchi, J. Stenhammar, R. J. Allen, D. Marenduzzo, and M. E. Cates, Scalar ϕ^4 field theory for active-particle phase separation, *Nat. Commun.* **5**, 4351 (2014).
- [59] R. Großmann, L. Schimansky-Geier, and P. Romanczuk, Active Brownian particles with velocity-alignment and active fluctuations, *New J. Phys.* **14**, 073033 (2012).
- [60] L. Caprini, U. M. B. Marconi, R. Wittmann, and H. Löwen, Active particles driven by competing spatially dependent self-propulsion and external force, *SciPost Phys.* **13**, 065 (2022).